Eur. J. Wood Prod. (2012) 70:407–413
DOI 10.1007/s00107-011-0573-8

ORIGINALS ORIGINALARBEITEN

Combination of X-ray and digital image correlation for the analysis of moisture-induced strain in wood: opportunities and challenges

Daniel Keunecke · Katia Novosseletz · Christian Lanvermann · David Mannes · Peter Niemz

Received: 15 December 2010 / Published online: 15 September 2011

Abstract In this present study, the moisture-induced deformation behaviour of a spruce sample was analysed one- and two-dimensionally with high resolution on the radial-tangential surface. For this purpose, an artificial speckle pattern was applied to the surface which was then recorded by a CCD camera during the deformation. The generated TIF images were analysed with a strain mapping software (VIC 2D) that computed the two-dimensional strain field from the surface deformation.

Selected options to evaluate two-dimensional data generated with X-ray imaging and digital image correlation are presented. Combining and correlating these techniques enables detailed analysis of structure-function relationships during swelling (and shrinkage) processes in wood. However, several issues still have to be solved to enhance effectiveness and user-friendliness of such investigations, as elucidated in detail in this paper.

Kombination von Röntgenmessung und digitaler Bildkorrelation zur Dehnungsanalyse an Holz: Potential und Schwierigkeiten

Zusammenfassung In dieser Arbeit wurde das feuchteinduzierte Deformationsverhalten einer Fichtenholzprobe ein- und zweidimensional mit hoher Auflösung auf der radial-tangentialen Probenoberfläche analysiert. Dazu wurde ein künstliches Specklemuster auf die Probenoberfläche aufgebracht, welches dann mit einer CCD-Kamera während der Deformation gefilmt wurde. Die generierten TIF-Dateien wurden mit einer Bildkorrelationssoftware (VIC 2D) ausgewertet, welche die zweidimensionalen Dehnungen auf der Probenoberfläche berechnete.

Es werden ausgewählte Möglichkeiten zur Auswertung zweidimensionaler Daten vorgestellt, die durch Röntgendurchstrahlung und digitale Bildkorrelation generiert wurden. Einerseits ermöglicht die Kombination und Korrelation dieser Techniken eine detaillierte Analyse von Struktur- Eigenschafts-Beziehungen während der Quell- (und Schwind-) Prozesse in Holz. Andererseits müssen noch einige Probleme gelöst werden, um die Effektivität und die Benutzerfreundlichkeit derartiger Untersuchungsmethoden zu verbessern, was in diesem Artikel im Detail beleuchtet wird.

D. Keunecke · C. Lanvermann (✉) · P. Niemz
Institute for Building Materials (Wood Physics), ETH Zurich, 8093 Zurich, Switzerland
e-mail: lanvermannchr@ethz.ch

K. Novosseletz
Faculty of Wood Sciences and Technology, Technical University in Zvolen, 96001 Zvolen, Slovakia

D. Mannes
Spallation Neutron Source Division (ASQ), Paul Scherrer Institute, 5232 Villigen, Switzerland

1 Introduction

Wood as a lightweight building material has many advantages over other materials. At the same time, its porous and hygroscopic character may appear to be a drawback since wood is susceptible to dimensional changes: a change in the ambient conditions, especially in the surrounding relative humidity, causes a change in the moisture content of the material which is accompanied by swelling or shrinkage. For European softwoods, for example, this is valid up to a wood moisture content of about 30%. Above this value, almost no dimensional changes take place.

Many moisture-related characteristics of wood are well known, such as the maximum or differential swelling co-

efficients. These parameters are usually mean values determined for the principal wood directions. Basically, this is sufficient for calculations (e.g., when wood is to be employed as an engineering material). It has to be taken into account, however, that moisture-related dimensional changes mainly depend on two structural parameters that can vary significantly in wood:

(1) *Density*. While the density of the orthotropic material wood is relatively constant in the longitudinal and tangential directions, a pronounced fluctuation is given along the radial direction within one growth ring (cf. Havimo et al. 2008). In domestic softwood species, the latewood (LW) density can be up to five times higher than the earlywood (EW) density. The most significant drop in density can be found at the LW-EW boundary. In ring-porous deciduous woods, the density differences between vessel-dominated and fibre-dominated tissue areas can also be considerable.

(2) *The microfibril angle (MFA)*. This parameter also varies strongly within one growth ring (see for example Reiterer et al. 1999); the MFA is commonly significantly smaller in the LW than in the EW of the same growth ring. The relatively high longitudinal swelling coefficient—compared to that of normal wood—particularly of compression wood with its high MFA is well known.

Several studies consider the impact of the anatomical composition on the response to the ambient conditions, such as that by Perré and Huber (2007). They determined the shrinkage of microscopic Norway spruce specimens from a saturated state, as immersed in water, to an air-dry state under a microscope and evaluated the data with an image processing algorithm.

The goal of this study here was to further develop this investigation by including the density: swelling processes were to be analysed on a growth ring level for areas of higher and lower density. This can contribute to a broad and detailed understanding of the underlying mechanisms and factors of macroscopic processes (e.g., in a wooden board or even in wooden composite materials) since the macroscopic behaviour usually can be ascribed to causes located on lower hierarchical levels.

This study was carried out on a small and clear spruce wood plate with relatively wide growth rings. Spruce, a softwood species with a very simple tissue structure, is well suited for such basic studies. In the case of deciduous woods, the interpretability is possibly complicated due to the multitude of cell types.

At first, the local density of this plate was determined with X-ray measurements. Then the plate was exposed to three consecutive steps of increasing air humidity. The corresponding swelling processes on the plate surface were recorded with a high-resolution camera, and the generated image files were analysed with digital image correlation (DIC) software, which can be regarded as a development of analogue photogrammetric techniques. In contrast to the usual measurement of dimensional changes, the DIC technique allows the evaluation of two-dimensional strain distributions.

Therefore, the informative value of such studies can clearly be increased by using DIC systems. Although well known for many years (Hild and Roux 2006; Pan et al. 2009), this technique was recently improved. Consequently, its operation became more user-friendly and software/hardware packages affordable. The system described in the following was used in diverse contexts by the authors' working group (e.g., Keunecke et al. 2008; Keunecke and Niemz 2008; Garab et al. 2010). A detailed description and analysis of the system can also be found in Valla et al. (2011).

The focus of this present paper is put on the methodological approach. Possibilities and problems of analysis are demonstrated as well as correlating density with deformation data. One-dimensional data profiles and full-field (two-dimensional) information are shown. Based on these results, the chosen methodological approach was critically assessed. Moreover, options to carry out future investigations are presented, as well as further possibilities to apply the chosen techniques, in particular with regard to practical applications.

2 Material and methods

In the present study, the local density and moisture-induced swelling behaviour of one Norway spruce (*Picea abies* [L.] Karst.) sample was analysed. The sample was cut to external dimensions of $40(R) \times 40(T) \times 5(L)$ mm^3. The growth rings were relatively wide, with an average in radial width of about 4.6 mm. The mean density of the sample was determined gravimetrically at room climate (about 20°C and 50% relative humidity (RH)). To obtain the local density within the radial-tangential plane of the specimen, X-ray transmission images were produced at the neutron imaging facilities of the Paul Scherrer Institute (Villigen, Switzerland) where the ambient atmosphere was again about 20°C and 50% RH (Mannes 2009). The specimen was placed in the beam path and exposed to the radiation (Fig. 1a) casting a shadow image onto the detector. The X-ray tube was operated at a voltage of 60 kV and the detector system was a combined scintillator-CCD camera system.

From the generated TIF image, the radial grey value distribution was extracted and copied into a spreadsheet program for further evaluation. The attenuation coefficient at each data point was calculated and multiplied with the sample mean density to calculate the local density according to Lambert-Beer's law (for further details see Keunecke et al. 2010).

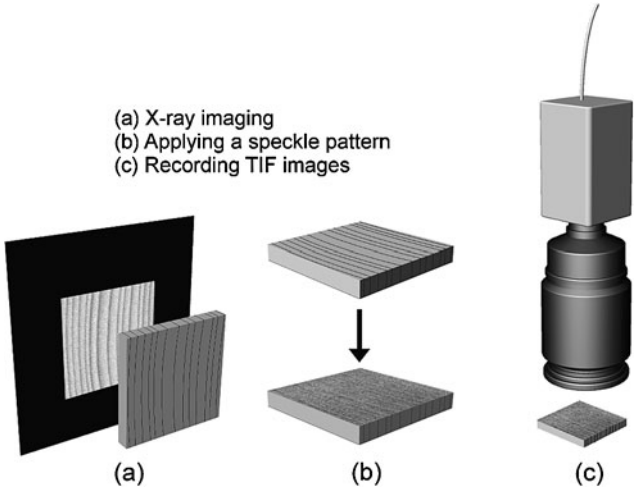

Fig. 1 Principle of the methodological approach
Abb. 1 Prinzip der methodischen Herangehensweise

Subsequently, the moisture content of the sample increased, and the respective swelling deformation was documented contact-free with a CCD camera and later evaluated with DIC software. The detailed procedure was as follows:

First, an artificial speckle pattern, consisting of white background paint and a randomly distributed black foreground, was applied with an airbrush gun (0.15 mm nozzle) on the monitored surface (the radial-tangential plane) of the sample (Fig. 1b). This pattern was needed for the evaluation of displacements on the specimen's surface by the strain mapping software. The layer of paint was thin enough to let the growth ring structure show through.

At this initial stage, the first digital image of the sample surface was recorded (Fig. 1c). The monochrome camera has a $2/3''$ CCD sensor with a 1392×1040 pixel array and is theoretically able to capture 15 frames per second with a minimal exposure time of 31 µs (which also makes it suitable for recording image series of samples undergoing quick deformation). The A/D converter of the camera has 12-bit and the interface to the computer is digital (FireWire). The optical axis of the camera was oriented perpendicular to the observed specimen surface. Then the specimen was exposed to 65% RH, and after reaching equilibrium moisture content, the next image was recorded and the sample was weighed again. This procedure was repeated a further two times (at 80% and 87% RH). Finally, the dry mass of the specimen was determined to calculate the wood moisture content assigned to the respective ambient humidity levels. In order to secure a good alignment of the individual pictures during the image acquisition process, the specimens were positioned on a rectangular mount under the camera. To monitor the ambient atmosphere, a data logger recording RH and temperature was placed adjacent to the samples.

The four resulting images were evaluated using the DIC software VIC 2D (Correlated Solutions Inc.). Its correlation algorithm is based on the principle of the allocation of an equal grey value pattern and therefore is able to track the displacement of small neighbourhoods. The first image was chosen as a reference image, and the in-plane strain distributions of the next three images were based on the undeformed reference image as the initial state (the out-of-plane movement was neglected). In this study, the focus is put on the strain along the radial wood direction. Strain profiles along lines as well as two-dimensional strain fields were analysed and visualised.

The two crucial parameters to be defined in the software are called *subset* and *step*. The subset defines the size of a grey value pattern in a defined neighbourhood around a central pixel. The software algorithm locates the best match between the reference pattern and the deformed pattern by maximising the cross correlation between two subsets. A subset of 21×21 pixels was used in this study. The measured displacement between is the average displacement of all pixels within the subsets. The step parameter defines the mesh width of a grid of pixels considered for calculation. A step of five (meaning the DIC process was performed for every 5th pixel in both the horizontal and vertical direction) was feasible in this study.

The area of interest (AOI) for evaluation was reduced to 26.5 mm × 25.8 mm. Precise and careful rotation and scaling procedures were applied to ensure the congruence of the TIF containing density information and the TIFs containing strain information. Eventually, the AOI was resolved with 266×259 (density) and 676×657 pixels (VIC 2D). Due to the chosen step parameter, fewer data points were generated by VIC 2D than by the X-ray approach. To facilitate comparability of the datasets, the VIC 2D data were then extrapolated and finally also presented as matrices of 266×259 data points.

3 Results and discussion

With 0.39 g/cm^3, the mean sample density determined gravimetrically is relatively low. This is a consequence of the wide growth rings: while the LW portion remains fairly constant in softwoods under good growth conditions, the EW portion increased, causing a lower overall density. The 2-dimensionally resolved X-ray measurements revealed density values between 0.2 and 0.9 g/cm^3, which correspond to the range from EW minima to LW maxima. This range is in good agreement with other literature sources (e.g. Wagenführ 2007).

The moisture-induced strain in the radial wood direction was analysed. The initial EMC corresponding to 20°C and 50% RH was 9.3% and increased to 11.7%, 14.7% and 18.0% as a result of storage under 20°C and 65%, 80%, and 87% RH, respectively. Assigning the mean radial strain determined with VIC 2D leads to fairly constant

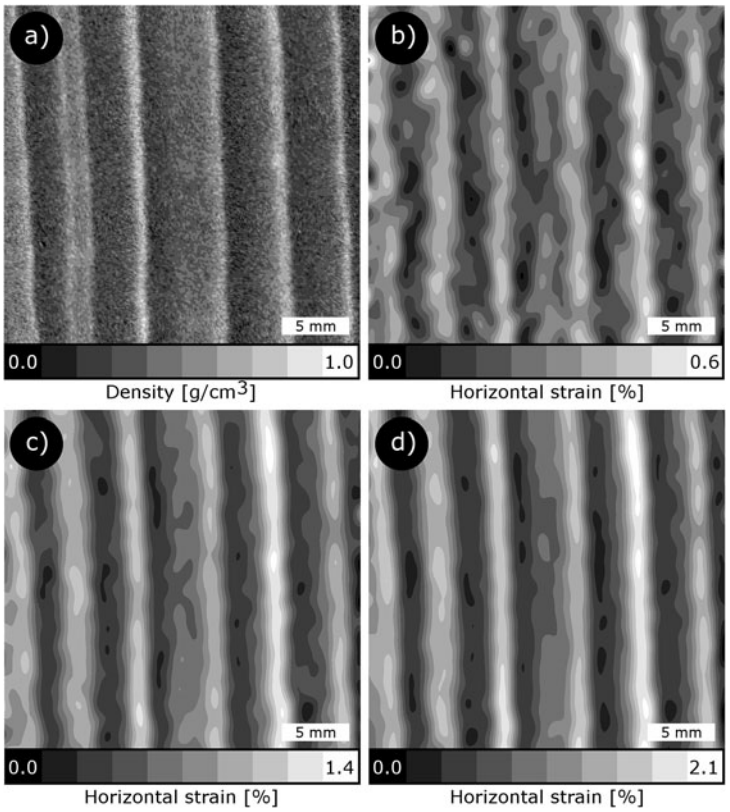

Fig. 2 Distribution of density (**a**) and horizontal strain (**b**)–(**d**) in the radial-tangential plane. Density is obtained as an integral over the specimen thickness, and strain reflects the surface deformation of the sample. (**b**)–(**d**) Show the strain (as developed by EMC) increase from 9.3% to 11.7% (**b**), 9.3% to 14.7% (**c**) and 9.3% to 18.0% (**d**)

Abb. 2 Verteilung von Dichte (**a**) und horizontaler Dehnung (**b**)–(**d**) in der radial-tangentialen Ebene. Die Dichte stellt einen integralen Wert (gemittelt über die Probendicke) dar, die Dehnung basiert auf der Oberflächendeformation des Prüfkörpers. (**b**)–(**d**) Zeigen die Dehnung, die sich eingestellt hat, nachdem die Ausgleichsfeuchte der Probe von 9,3 % auf 11,7 % (**b**), von 9,3 % auf 14,7 % (**c**) und von 9,3 % auf 18,0 % (**d**) angestiegen ist

differential swelling coefficients of 0.11 to 0.12 %/% (percent swelling per percent increase of wood moisture content). This is about one third lower than the values stated by e.g. Niemz (1993); besides the generally high variance of physical-mechanical wood properties, this can certainly be ascribed to the relatively low density of the sample.

The power of DIC techniques, however, is the ability to resolve phenomena such as strain locally. Due to the laminate-like character of wood in the radial direction (where low- and high-density layers alternate), the relationship between local density and local moisture-induced strain is particularly interesting. In principle, two expedient options would be (1) to carry out two-dimensional strain analysis on the specimen surface or a subarea of it or (2) to reduce evaluation to a line or a small band running parallel with the radial wood direction.

The two-dimensional analysis is shown in Fig. 2 for an area of 26.5 mm × 25.8 mm as described above. The corresponding density information (Fig. 2a) of the sample at an EMC of 9.3% clearly shows the small LW bands (bright pixels) and the darker EW and transition wood regions. From the grey value distribution, the growth direction can be derived (from left to right in Fig. 2a). Figures 2b–2d show the horizontal strain of the specimen (in the radial wood direction) as developed by EMC increases from 9.3% to 11.7% (Fig. 2b), 9.3% to 14.7% (Fig. 2c) and 9.3% to 18.0% (Fig. 2d). Since moisture-induced strain largely depends on the wood density, the strain in the denser LW bands is much higher than in EW. It is clearly visible that this spread is more pronounced the higher the EMC is. It is also apparent that at lower EMCs (Fig. 2b), the vertical strain bands still have a more spotty character, while with increasing EMC, a clear vertical orientation of these bands develops (Fig. 2d).

This separation between areas of low and high strain, however, is less sharp than what one would expect from the 2-dimensional density distribution illustration (Fig. 2a). This is a consequence of data processing with the DIC software and depends on the chosen subset size and step parameters: with increasing subset the displacement is averaged over a larger area (subset) and this leads to a more smoothed dataset. A certain averaging and thus smoothing cannot be avoided since it is a basic principle of DIC, which is only possible with a certain subset size and this inevitably causes averaging. Smoothing also increases with increasing step parameter, as the number of evaluated data points within the image decrease. The challenge when working with DIC software is to find a good compromise between smoothing, spatial resolution, random noise, computing time and realistic absolute values (cf. Valla et al. 2011).

The confrontation of the data is shown in Fig. 3 where strain and smoothed density are plotted over the measurement points. It has to be mentioned that the density data have been smoothed according to the subset size to offer a prefer-

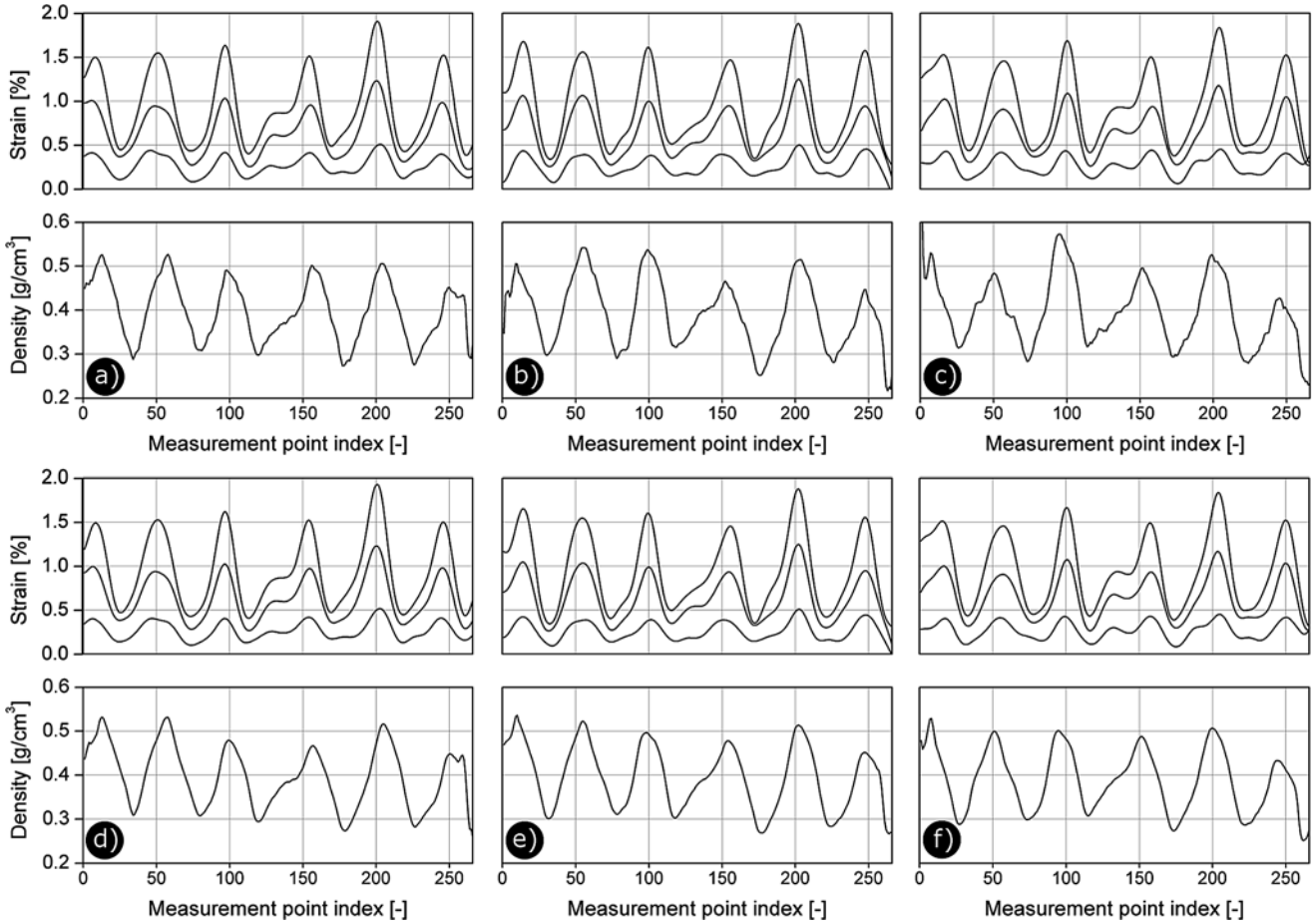

Fig. 3 Strain and density plotted over the measurement points. (**a**)–(**c**) Show data profiles of one horizontal row of data from the 2-dimensional matrix: in (**a**) row 65 is shown, in (**b**) row 130, and in (**c**) row 195 (of a total of 259 horizontal data rows). The *three curves* in *each* of the *upper diagrams* represent the strain corresponding to the respective EMC levels. (**d**)–(**f**) Show the result of a further smoothing applied on the columns of the data matrices. The average curve of 21 horizontal rows of data was taken into account (in (**d**) the mean of rows 55 to 75 is shown, in (**e**) the mean of rows 120 to 140, and in (**f**) the mean of rows 185 to 205)

Abb. 3 Dehnung und Dichte in Abhängigkeit von den Messpunkten. (**a**)–(**c**) Zeigen Datenprofile einer horizontalen Datenreihe einer 2-dimensionalen Datenmatrix: (**a**) Zeigt Datenreihe 65, (**b**) Datenreihe 130, und (**c**) Datenreihe 195 von insgesamt 259 horizontalen Datenreihen. Die *drei Kurven* der *jeweils oberen Diagramme* zeigen die Dehnung der jeweiligen Ausgleichsfeuchteniveaus. (**d**)–(**f**) Zeigen das Ergebnis einer weiteren Glättung der Datensäulen in den Matrizen. Die Mittelwertkurve von 21 horizontalen Datenreihen wurde ermittelt: (**d**) zeigt die Mittelwertkurve der Datenreihen 55–75, (**e**) die Mittelwertkurve der Datenreihen 120–140 und (**f**) die Mittelwertkurve der Datenreihen 185–205

ably good comparability. The curves in Figs. 3a–3c show data profiles of only one single horizontal row of data from the whole 2-dimensional data matrix: in Fig. 3a, data row 65 is shown, in Fig. 3b data row 130, and in Fig. 3c data row 195 (of a total of 259 horizontal data rows). The three strain curves in each of the upper diagrams represent the strain corresponding to the respective EMC (of course with the upper curve belonging to the highest EMC). The peaks of strain and density profiles are highly congruent, demonstrating the strong density dependence of strain. The coefficient of determination of the regression line between the three pairs of matrices (strain at 11.7% EMC and smoothed density, strain at 14.7% EMC and smoothed density; strain at 18.0% EMC and smoothed density) was about 0.80 (and about 0.72 when density was unsmoothed).

Figures 3d–3f show the result of further smoothing, this time applied to the columns of the data matrices. Instead of one single horizontal row of data, the average curve of 21 horizontal rows of data was taken into account (in Fig. 3d, the mean of data rows 55 to 75 is shown, in Fig. 3e the mean of data rows 120 to 140, and in Fig. 3f the mean of data rows 185 to 205). The effect of this second smoothing procedure is more noticeable for density than for strain. This is due to the above-mentioned fact that the DIC strain data were already smoothed by the software while density data read out of the X-ray-generated TIF files can be seen as unmodified data.

The evaluation procedure described so far is rather a qualitative than a quantitative approach. Certain patterns of correlation between density and strain datasets are highly vis-

ible, but a mathematical approach would certainly increase the informative value of such investigations. Using DIC software, such as VIC 2D, generally offers large potential in the field of wood research, as outlined in the following:

- The 2-dimensional analysis of surface deformation enables a much deeper analysis of structure-property relationships in wood on the growth ring level and below than methods integrating the behaviour over the specimen thickness or width. This is particularly relevant for wood since it is strongly anisotropic regarding its structure and behaviour, and since it can be regarded as a laminated material in the radial direction due to the EW and LW bands. Investigating moisture-induced strain is only one of many possible applications. Another interesting question that could be approached with DIC analysis is: what is the difference between the radial elastic modulus of EW and LW tissue?
- In many studies, a qualitative approach resulting in rough information on strain distribution is entirely sufficient, e.g., to analyse if stress distribution is symmetric or asymmetric, or to predict where crack initiation or propagation will take place.
- The effort to supplement experiments with DIC is relatively small, and the capacity and performance of today's computers makes results quickly available. The graphical user interface and the export functions of commercial DIC software have been improved and adapted to users' demands in recent years.
- Besides vertical and horizontal strain, further data provided by DIC software include, for example, the major principal strains, shear strains, velocity variables (deformation or strain over time) and the confidence interval for the match at a certain point. Moreover, diverse useful options, such as post processing of data, are available.

On the other hand, combining and comparing datasets generated with a DIC technique and, as in this study, with an X-ray facility raises some difficulties:

- DIC data result from the surface deformation of a material while density data represent the integral of a sample with a certain thickness. These datasets do not necessarily have to be congruent. The quality of the density data largely depends on the accurateness of the specimen preparation and on the anatomical structure of the sample. The best results can be achieved when the X-ray beam is absolutely parallel with the longitudinal wood direction. Due to the somewhat irregular tissue composition of wood, only an approximation is possible. Analysis of transmission measurements in the tangential direction is complicated due to the curvature of growth rings, and aligning the beam parallel to the radial wood direction is pointless since low- and high-density layers alternate and superpose each other. Besides the specimen alignment, ensuring an absolutely constant sample thickness is crucial towards producing reliable density data.
- Synchronising datasets manually is a laborious procedure. To automate this, a professional numerical computing environment including matrix manipulations and implementation of algorithms would be useful. It could help in making the desired processes (scaling, rotation, edge and corner detection) more effective and comfortable.
- The users of DIC software should be aware of the fact that the generated data have undergone a certain smoothing procedure resulting in datasets with cropped peaks. Thus the users should be careful when using the smoothed data to derive mathematical relationships. This is the reason why the authors did not express the density-dependent moisture-induced radial strains by a mathematical equation. Furthermore in the case of wood, smoothing, for example, can result in the sharp density drop at the growth ring boundary not being correctly reflected in the data. A likewise smoothing of the corresponding dataset—in this particular case the density—is not ideal since the real behaviour and structural properties are blurred. This can result in erroneous conclusions if the data are further processed, e.g., when the material behaviour is numerically modelled. Avoiding the smoothing completely is not possible, thus the aim of the approach must be to minimize the resulting error. To achieve this, the artificially applied speckle pattern can be optimized to allow for downsizing the subset parameter resulting in higher resolution. Moreover, the chip of the digital camera should be used to full capacity by omitting the unneeded margin encasing the AOI or higher resolution cameras. Unnecessary movements of the sample during recording of a series of images should also be avoided since this can also reduce the subset size. And finally, using wood samples with relatively wide growth rings (like the sample in this present study) can reduce the influence of smoothing on the results. This, of course, is particularly valid when studies in the radial wood direction are the focus of interest.

Taking the mentioned aspects and recommendations into account in future investigations can help improve the currently used methodological approach to synchronise datasets and thus can contribute to a higher informative value of the results and conclusions derived from the generated data.

4 Conclusion

With certain restrictions, the chosen methodological approach proved to be suitable to correlate local density with local deformation data. Therefore, this combination of techniques can be a promising step towards evaluating structure-property relationships. Currently, the inconvenient process

of synchronizing X-ray and DIC images is still unsatisfying. Developing a user-friendly solution, however, should be possible in principle. By using appropriate software able to work with filter algorithms or to recognize patterns provides the potential to facilitate the first basic step of raw data preparation.

Besides the proposed research question, the chosen approach of course is predestined to focus on further basic research questions within the field of wood:

- Besides softwood species, the material behaviour of deciduous woods, particularly of ring-porous species with their local density variations, could be interesting.
- Furthermore, investigating the off-axis deformation behaviour of wood (between its principal axes) could provide further valuable information on the material behaviour (e.g., about the shear deformation in the radial-tangential plane).
- In a uniaxial tension or compression test with the load axis parallel to the radial wood direction, the local radial modulus of elasticity (MOE) could be determined via digital image correlation, i.e., the EW and LW MOE could be calculated separately. This is an interesting concept when regarding wood as a sandwich material composed of layers with different properties along the radial direction. Also the collapse, e.g., of EW (flattening of cells of rows of cells during drying of pressure treatment; Bucur 2011) could be observed.
- The response of wood to densification could be analysed (Haller and Wehsener 2004).
- Additional mapping of further local properties (such as the MFA) could extend the structure-property relationships on other anatomical features.

A possible practical application could be the industrial analysis and observation of wood deformation as a result of technical drying (shrinkage can be analysed as well). Of course, all the suggestions mentioned in principle are also transferable to other materials with local inhomogeneities.

References

Bucur V (ed) (2011) Delamination in wood, wood products and wood-based composites. Springer, Dordrecht

Garab J, Keunecke D, Hering S, Szalai J, Niemz P (2010) Measurement of standard and off-axis elastic moduli and Poisson's ratios of spruce and yew wood in the transverse plane. Wood Sci Technol 44(3):451–464

Havimo M, Rikala J, Sirvio J, Sipi M (2008) Distributions of tracheid cross-sectional dimensions in different parts of Norway spruce stems. Silva Fenn 42(1):89–99

Haller P, Wehsener J (2004) Mechanical properties of densified spruce. Holz Roh- Werkst 62(6):452–454

Hild F, Roux S (2006) Digital image correlation: from displacement measurement to identification of elastic properties—a review. Strain 42(2):69–80

Keunecke D, Hering S, Niemz P (2008) Three-dimensional elastic behaviour of common yew and Norway spruce. Wood Sci Technol 42(8):633–647

Keunecke D, Niemz P (2008) Axial stiffness and selected structural properties of yew and spruce microtensile specimens. Wood Res 53(1):1–14

Keunecke D, Mannes D, Niemz P, Lehmann E, Evans R (2010) Silviscan vs. neutron imaging to generate radial softwood density profiles. Wood Res 55(3):49–60

Mannes D (2009) Non-destructive testing of wood by means of neutron imaging in comparison with similar methods. Dissertation, ETH Zurich

Niemz P (1993) Physik des Holzes und der Holzwerkstoffe. DRW, Leinfelden-Echterdingen

Pan B, Qian KM, Xie HM, Asundi A (2009) Two-dimensional digital image correlation for in-plane displacement and strain measurement: a review. Meas Sci Technol 20(6)

Perré P, Huber F (2007) Measurement of free shrinkage at the tissue level using an optical microscope with an immersion objective: results obtained for Douglas fir (*Pseudotsugamenziesii*) and spruce (*Picea abies*). Ann Sci For 64(3):255–265

Reiterer A, Lichtenegger H, Tschegg S, Fratzl P (1999) Experimental evidence for a mechanical function of the cellulose microfibril angle in wood cell walls. Philos Mag A 79(9):2173–2184

Valla A, Konnerth J, Keunecke D, Niemz P, Müller U, Gindl-Altmutter W (2011) Comparison of two optical methods for contactless, full field and highly sensitive in plane deformation measurements using the example of plywood. Wood Sci Technol, doi:10.1007/s00226-010-0394-7

Wagenführ R (2007) Holzatlas. Fachbuchverlag im Carl Hanser Verlag, Leipzig